





# Vitality of autologous retromolar bone grafts for alveolar ridge augmentation after a 3-months healing period: A prospective histomorphometrical analysis

Andres Stricker<sup>1</sup>  | Tobias Fretwurst<sup>1</sup>  | Arzu Abdullayeva<sup>1</sup> | Dieter Bosshardt<sup>2,3</sup> | Tara Aghaloo<sup>4</sup>  | Fabian Duttenhöfer<sup>1</sup> | Luca Cordaro<sup>5</sup>  | Katja Nelson<sup>1</sup> | Christian Gross<sup>1</sup>

<sup>1</sup>Department of Oral- and Craniomaxillofacial Surgery/Translational Implantology, Faculty of Medicine, Medical Center, University of Freiburg, Freiburg im Breisgau, Germany

<sup>2</sup>Department of Periodontology, School of Dental Medicine, University of Bern, Bern, Switzerland

<sup>3</sup>Robert K. Schenk Laboratory of Oral Histology, School of Dental Medicine, University of Bern, Bern, Switzerland

<sup>4</sup>Section of Oral and Maxillofacial Surgery, UCLA School of Dentistry, Los Angeles, California, USA

<sup>5</sup>Department of Periodontics and Prosthodontics, Policlinico Umberto I, Eastman Dental Hospital, Rome, Italy

## Correspondence

Andres Stricker, Department of Oral- and Craniomaxillofacial Surgery/Translational Implantology, Faculty of Medicine, Medical Center, University of Freiburg, Hugstetter Straße 55, D-79106 Freiburg, Germany.

Email: [andres.stricker@uniklinik-freiburg.de](mailto:andres.stricker@uniklinik-freiburg.de)

## Funding information

Geistlich Pharma

## Abstract

**Objectives:** The incorporation of retromolar bone grafts used for alveolar ridge augmentation is not well understood. This prospective observational study aims to supply histomorphometrical data from bone graft biopsies taken at the time of retrieval and after a 3-month healing period using patient-matched biopsies.

**Materials and Methods:** In 17 patients, trephine biopsies of the graft were acquired at the time of graft retrieval and after a 3-month healing period. The biopsies were compared histomorphometrically regarding the number of osteocytes, appearance of osteocyte lacunae, quantity, surface area, and activity of the Haversian canals.

**Results:** All grafts appeared clinically stable after screw removal and 17 implants were placed. Histomorphometric analysis revealed no significant difference in the number of osteocytes ( $p = .413$ ), osteocyte lacunae ( $p = .611$ ), the ratio of filled/empty osteocyte lacunae ( $p = .467$ ) and active Haversian canals ( $p = .495$ ) between the biopsies retrieved after a 3-months healing period with those at the time of grafting. The only significant difference was noted in the mean surface area of the Haversian canals ( $p = .002$ ). Specifically, the grafts post 3-month healing showed a significantly larger mean area ( $0.069 \text{ mm}^2$ ) compared to the time of grafting ( $0.029 \text{ mm}^2$ ).

**Conclusion:** This study demonstrates, compared to other data, a high rate of vital structures in retromolar bone block grafts after 3 months of healing, exhibiting the same histological features in comparison to the biopsies from the native alveolar ridge. Standard histomorphometrical parameters, e.g., the amount of filled or empty osteocyte lacunae for the description of the vitality of the graft need to be reappraised.

## KEYWORDS

autologous, bone graft, haversian canal, osteocyte lacunae, osteocytes, retromolar

This is an open access article under the terms of the [Creative Commons Attribution-NonCommercial-NoDerivs](https://creativecommons.org/licenses/by-nc-nd/4.0/) License, which permits use and distribution in any medium, provided the original work is properly cited, the use is non-commercial and no modifications or adaptations are made.

© 2024 The Author(s). *Clinical Oral Implants Research* published by John Wiley & Sons Ltd.

## 1 | INTRODUCTION

It is estimated that nearly half of all dental implant procedures necessitate bone grafting due to inadequate dimensions of the alveolar bone (Cha et al., 2016). To address major-sized vertical or horizontal defects, several bone grafting methodologies have been established (Fretwurst, Gad, et al., 2015; Fretwurst, Nack, et al., 2015). Currently, various bone substitutes are available (Fretwurst et al., 2014; Yamada & Egusa, 2018). However, only autologous bone grafts exhibit osteoconductive, osteoinductive, and osteogenic properties and, thus, maintain their status as the gold standard for vertical and major horizontal alveolar bone reconstruction (Sakkas et al., 2017; Sanz & Vignoletti, 2015). Intraoral bone grafts from the posterior ramus mandibulae/retromolar region are favored due to their easy access and low harvesting morbidity compared to extraoral bone grafts (Nkenke & Neukam, 2014). Implants placed in the jawbone augmented with intraoral bone grafts show success rates exceeding 85% and implant survival rates of more than 90% (Aloy-Prosper et al., 2015; Clementini et al., 2011; Esposito et al., 2009). The posterior mandibular ramus/retromolar region is currently the preferred site for harvesting intraoral bone grafts, as grafts from other intraoral locations have been associated with increased complications, including postoperative pain and altered sensation or vitality of adjacent teeth (Nkenke & Neukam, 2014; Reissmann et al., 2013; Starch-Jensen et al., 2020).

Although retromolar bone grafts are used with excellent clinical success, little is known about their mode of incorporation at the recipient site. To date, only limited studies have performed histologic analysis of human, incorporated retromolar bone grafts (Acocella et al., 2010; Burger et al., 2011; Buser et al., 1996; Spin-Neto et al., 2014, 2015; Wang et al., 2023). However, their study modalities were heterogeneous due to different healing periods (3–13 months), comparison of different bone graft configurations (cortical, corticocancellous) and grafting techniques (1 vs. 2 screws). All these studies have found clinical success of the bone grafting. The histologic success was assessed by discriminating areas of bone with filled osteocyte lacunae (vital) from necrotic areas. Osteocyte lacunae without a histologically visible osteocyte were termed empty osteocyte lacunae, and the bone areas comprising them were declared non-vital/necrotic, as described in early histologic studies of bone (Frost, 1960). The reported fraction of necrotic bone ranged from under 10% (Burger et al., 2011) to over 80% (Acocella et al., 2010). To date, the retromolar bone graft at the time of retrieval was never compared histologically to the incorporated graft to investigate how the graft vitality evolves during incorporation.

In the complex process of bone graft incorporation, which is determined by the host-graft union, revascularization, and new bone formation, the vitality and viability of the osteocytes depend on the nutritive supply provided by the adjacent vasculature (Chen et al., 1994; Cypher & Grossman, 1996). As the center of the osteon, the Haversian canal serves as a guide for vessel formation. It is also proposed to be the site of bone remodeling. Around the

Haversian canal, it can be differentiated between newly formed, nonmineralized bone matrix (osteoid) and mature, mineralized bone matrix (Maggiano et al., 2016). The grade of bone matrix mineralization around a Haversian canal implies a specific cellular activity dominated by osteoclasts, osteoblasts, and the osteocyte lacuno-canalicular network, as indicated by recent research (Ayoubi et al., 2021). Histological studies revealed variations in the appearance of Haversian canals, which can appear empty and lack a seam of new osteoid in areas of necrotic bone (Marx & Tursun, 2012). It is known that new bone formation is initiated from the Haversian canal, although a standardized terminology is missing to describe the activity at the Haversian canals (Lassen et al., 2017). The present study adopts a distinction between “active” Haversian canals (filled and encircled by new osteoid) and “inactive” Haversian canals (empty and encased by mineralized bone matrix) to obtain a further parameter to assess the vitality of the bone graft.

This study aimed to assess and compare the vitality of the retromolar bone graft both at the time of retrieval from the donor site and post-incorporation following a 3-month healing period. Histomorphometry was utilized to address the presence of osteocytes and their lacunae, as well as to assess the activity and morphology of Haversian canals, using patient-matched biopsies.

## 2 | MATERIALS AND METHODS

The protocol was approved by the ethics committee of the Albert-Ludwigs-University Freiburg, Germany (Protocol number 138/14) and followed the STROBE guidelines (<https://www.equator-network.org/reporting-guidelines/strobe/>). All patients were treated in accordance with the Helsinki Declaration of 1964, as revised in 2013.

### 2.1 | Patient cohort

Individuals included in this prospective observational study were patients aged over 18 years requiring intraoral horizontal bone grafting prior to dental implant placement. Eligible participants with single tooth gap or partially edentulous according to Terheyden classification 2/4 were healthy, nonsmokers, with no general contraindications for bone block grafting (Cordaro & Terheyden, 2014; Terheyden, 2010). Patients were excluded if they were undergoing antiresorptive, radio-, or chemotherapy; currently pregnant or nursing; had a history of malignancy; or had general diseases that could potentially affect bone or connective tissue homeostasis.

### 2.2 | Surgical procedure and sample retrieval

Full-thickness intraoral onlay grafting and implant placement were executed by an experienced surgeon (A.S.) under local anesthesia

(Ultracain® D-S forte, Aventis Pharma, Frankfurt, Germany), adhering to a standardized protocol.

The bone graft was harvested from the retromolar region of the lower jaw, involving a crystal incision with vertical releasing incisions and preparation of a mucoperiosteal full-thickness flap. Piezosurgery was employed to outline the graft. During the removal and shaping of the cortical bone block from the mandibular ramus, the first sample

(Pre-Tx=pre-transplantation/native bone) was secured using a trephine bur ( $\varnothing$  1.5 mm internal; Zepf, Tuttlingen, Germany) (Figure 1a).

The bone block was placed with no vertical overlap and then tightly fitted by two titanium lag screws of 1.2- or 1.5-mm diameter and 8-mm length (Bone Fixation Aesculap, Tuttlingen, Germany) at the pristine recipient site in either the upper or lower jaw. No autologous chips were used to fill the minimized gap.

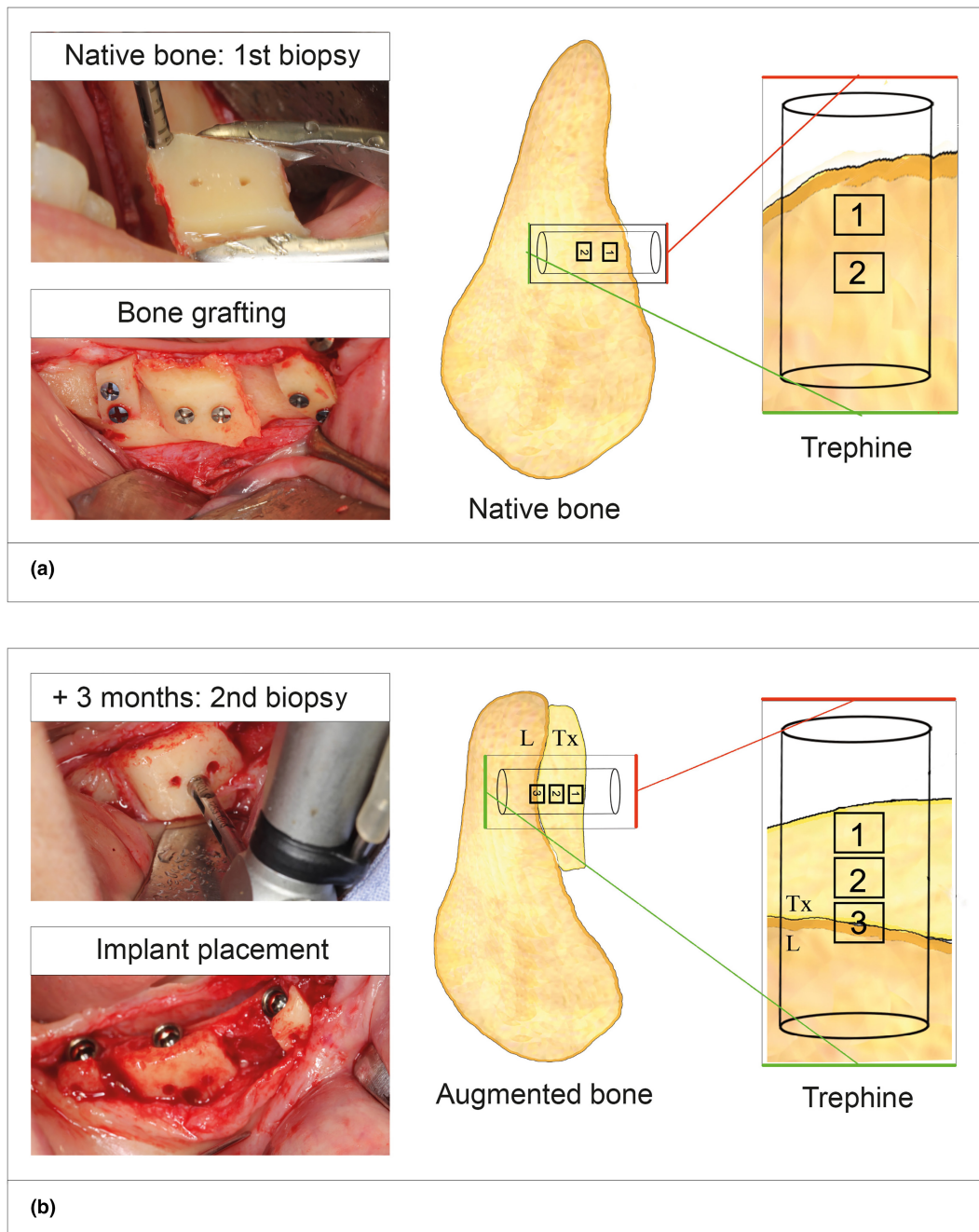


**FIGURE 1** Transversal bone biopsy retrieval. (a) The initial bone biopsy retrieval with a trephine ( $\varnothing$  1.5 mm) during bone grafting from the mandibular ramus. (b) The second biopsy retrieval before implant placement after 3 months of graft healing from the same block and patient with the same trephine diameter. The right side of the figure illustrates the location of the ROIs within the trephine. L, local/resident bone; Tx, Transplant/Graft.

Subsequently, tension-free wound closure was attained with non-resorbable sutures (Seralon 5.0, Serag Wiessner, Germany) following a periosteal-releasing incision.

After a 3-month healing period, re-entry was conducted. A transversal trephine sample ( $\varnothing$  1.5 mm internal; Zepf, Tuttlingen, Germany) harvested under sterile saline cooling with a rotation speed of 600 rpm was retrieved from the integrated graft, which included the transplanted graft and a part of the resident bone beneath it (Post-Tx = post-transplantation/incorporated bone graft after three months), preceding the implant placement per the manufacturer's protocol (Straumann, Basel, Switzerland) (Figure 1b). Tension-free closure of the flaps was performed with non-resorbable sutures (Seralon 5.0, Serag Wiessner, Germany). We did not measure the ridge width or height during re-entry.

## 2.3 | Histological procedure

Immediately after retrieval, the bone cores with the trephine bur were fixed in 10% formalin, preserving the oral facial orientation of the bone during histological processing. All specimens were left undecalcified and dehydrated in increasing concentrations of ethanol and embedded in methylmethacrylate. Serial sections of ~500 microns in thickness were cut using a low-speed diamond saw with coolant (Varicut® VC-50, Leco, Munich, Germany). After mounting the sections onto acrylic glass slabs, they were ground and polished to a final thickness of about 100  $\mu$ m (Knuth-Rotor-3, Struers, Rodovre/Copenhagen, Denmark). The sections were stained with Pararosanolin (Sigma, Merck) and Azure II (Merck) staining as described by (Lasckó & Lévai, 1975). The sections were digitized with a ProgRes® C5 digital camera (Jenoptik Laser, Optik Systeme GmbH, Jena, Germany) connected to a Zeiss Axioplan microscope (Carl Zeiss, Göttingen, Germany).

## 2.4 | Histomorphometry

The Pre-Tx and Post-Tx trephine samples from each patient were compared histomorphometrically. The ROI size was determined as 0.75  $\times$  0.75 mm (length  $\times$  width). ROI 1: buccal/outer portion of the graft; ROI 2: inner portion of the graft (Figures 1 and 2); ROI 3: interfacial zone (the area corresponding to the connection of the graft to the recipient site). The histomorphometry was performed with ImageJ (Rasband WS, ImageJ, U.S. National Institutes of Health, Bethesda, MD, USA). The following parameters were analyzed within the ROIs: 1. Quantity of osteocyte lacunae, 2. Quantity of osteocytes, 3. Percentage of filled osteocyte lacunae (number of osteocytes to number of osteocyte lacunae), 4. Quantity of Haversian canals, 5. Quantity of active Haversian canals (surrounded by new bone formation), 6. Surface area of Haversian canals. Haversian canals that showed a seam area of newly formed osteoid, which can be discriminated by the

intensive red coloration around the canal lumen, were marked as "active" (Figure 2).

## 2.5 | Statistics

The normal distribution of the result values was tested graphically and statistically (Shapiro–Wilk test). Descriptive/Explorative statistics, nonparametrical statistical hypothesis tests (Kruskal–Wallis, Mann–Whitney *U*, ANOVA) with posthoc testing (Bonferroni) were performed using IBM SPSS Statistics for Macintosh, version 28 (IBM Corp., Armonk, N.Y., USA). *p*-Values  $\leq$  .05 were considered statistically significant.

No statistical evaluation was performed for the ROI 3.

## 3 | RESULTS

Seventeen patients were included in the study (6/17 male; 11/17 female; age:  $\varnothing$  60,8  $\pm$  10,6 years). The bone grafting procedure was uneventful, without dehiscence in all patients. The entire surface of the graft appeared vascularized (Figure 2). After screw removal the grafts were clinically stable and 17 implants were successfully placed. The grafts were transplanted into the molar and premolar regions of the mandible (molar: 10/17, premolar: 3/17, front: 1/17). Conversely, three grafts were transplanted into the maxilla (front: 2/17, premolar: 1/17). Due to individual sample morphology and size, not every sample was suitable for setting all three ROIs (*N* Pre-Tx ROI = 17, *N* Pre-Tx ROI 2 = 12, *N* Post-Tx ROI 1 = 17, *N* Post-Tx ROI 2 = 16, *N* Post-Tx ROI 3 = 7). No inflammatory cells were detectable in any biopsy after grafting. The results are visualized in Figures 3 and 4. All *p*-values and standard descriptive statistics are given in Table A1 in Appendix. As follows, the results were extrapolated to 1 mm<sup>2</sup>.

### 3.1 | Osteocyte and Haversian Canal pattern pre-Tx vs post-Tx

When pooling the results of ROI 1 and 2 for each sample and comparing the Pre-Tx and Post-Tx samples, Post-Tx bone featured a significantly higher mean surface area of the Haversian canal (mean = 0.069 mm<sup>2</sup>) than Pre-Tx samples (mean = 0.029 mm<sup>2</sup>), *p* = .002 (Figure 4b). No significant differences were found between the Pre-Tx and Post-Tx bone samples regarding the number of osteocytes (Pre-Tx mean = 143.36/mm<sup>2</sup>, Post-Tx mean = 161.19/mm<sup>2</sup>, *p* = .413, Figure 3a), the number of osteocyte lacunae (Pre-Tx mean = 276.46/mm<sup>2</sup>, Post-Tx mean = 271.97/mm<sup>2</sup>, *p* = .611, Figure 3b), ratio of filled/empty osteocyte lacunae (Pre-Tx mean = 55,2%, Post-Tx mean = 59,8%, *p* = .467, Figure 3d), number of Haversian canals (Pre-Tx mean = 8.96/mm<sup>2</sup>, Post-Tx mean = 7.48/mm<sup>2</sup>, *p* = .074), and the number of active Haversian canals (Pre-Tx mean = 6.18/mm<sup>2</sup>, Post-Tx mean = 5.84/mm<sup>2</sup>; *p* = .495, Figure 4a).



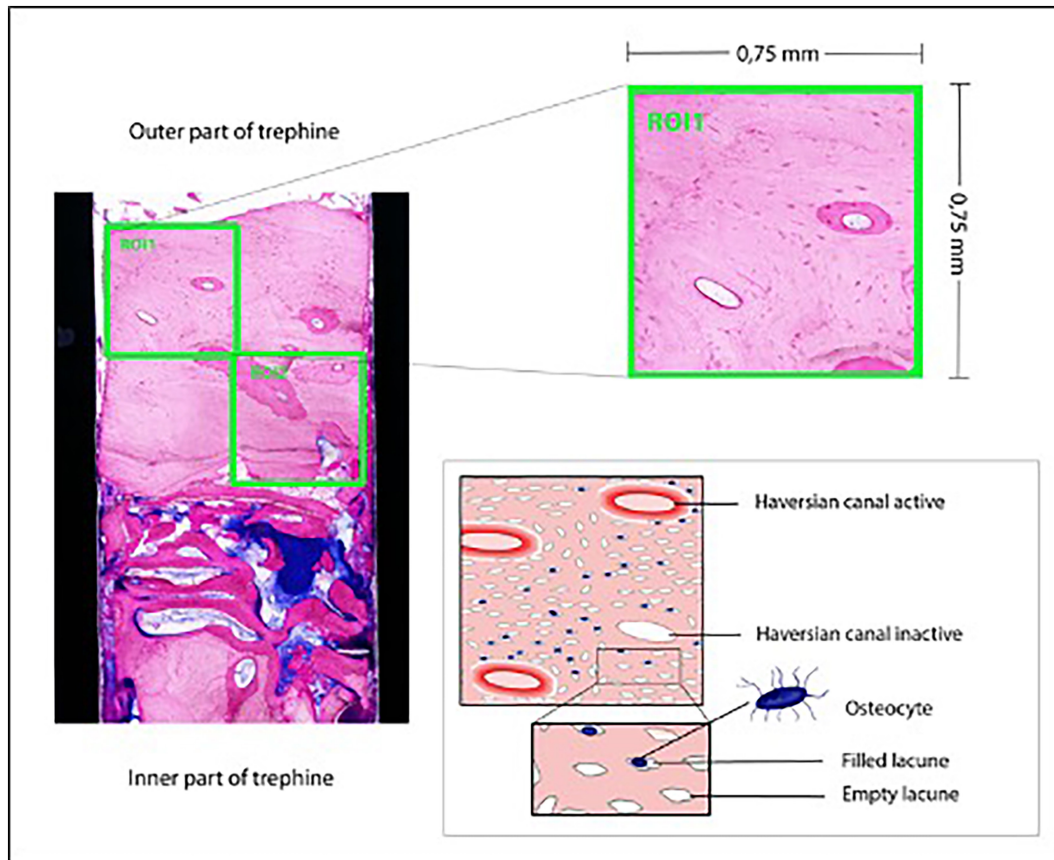


**FIGURE 2** Histomorphometry. The left side of the figure shows an exemplary section of an incorporated bone block after 3 months of healing (Pararosanilin Azur II). The right upper part of the figure shows an exemplary ROI 1 with an active and inactive Haversian canal. The right lower part of the figure illustrates schematic examples of active and inactive Haversian canals and filled and empty osteocyte lacunae.

### 3.2 | Qualitative analysis of the interfacial zone (ROI 3)

It was of particular interest to investigate how the border zone between the resident (local) and the transplanted bone block was structured (Figure 5a). In all biopsies, Howship's lacunae with new bone on top were seen on both sides of the border zone, i.e. on the local and the transplanted bone (Figure 5b). The border zone itself consisted of newly formed trabecular bone connecting the two bone parts (Figure 5b). This continuity could not be clearly demonstrated in all biopsies because drilling with the hollow drill can easily cause mechanical damage to the fragile newly formed trabecular bone. In addition to smaller fractures, small pieces of bone particles (debris) were also pushed from the edge of the hollow drill into the interior of the biopsies.

### 3.3 | Comparison of ROI 1 with ROI 2

The comparison of the different ROIs of the Pre-Tx and Post-Tx bone samples demonstrated the same trends as with pooled ROIs, however, with more restrictive significances due to posthoc testing (see differences regarding the Haversian canal area in Figure 4b,c).

No significant differences were found between ROI 1 and ROI 2 within the bone grafts at Pre-Tx and at Post-Tx for any investigated parameter.

## 4 | DISCUSSION

The study aimed to compare histological characteristics of retromolar bone block grafts taken at the time of grafting and after three months of healing within the same patient.

The primary finding of the study is that retromolar bone grafts after three months of healing exhibit the same histological features in comparison to the native alveolar ridge. Comparing the histological patterns of osteocytes and Haversian canals between Pre-Tx and Post-Tx bone samples, no significant differences were demonstrated in terms of the number of osteocytes, the number of osteocyte lacunae, the ratio of filled/empty osteocyte lacunae, the number of Haversian canals, and the number of active Haversian canals. The sole distinction observed was an increase in the mean Haversian canal area in the Post-Tx bone (mean = 0.069 mm<sup>2</sup>) compared to the Pre-Tx samples (mean = 0.029 mm<sup>2</sup>).

Our study, involving iliac crest grafting with a three-month healing period, demonstrated excellent results, prompting us to choose

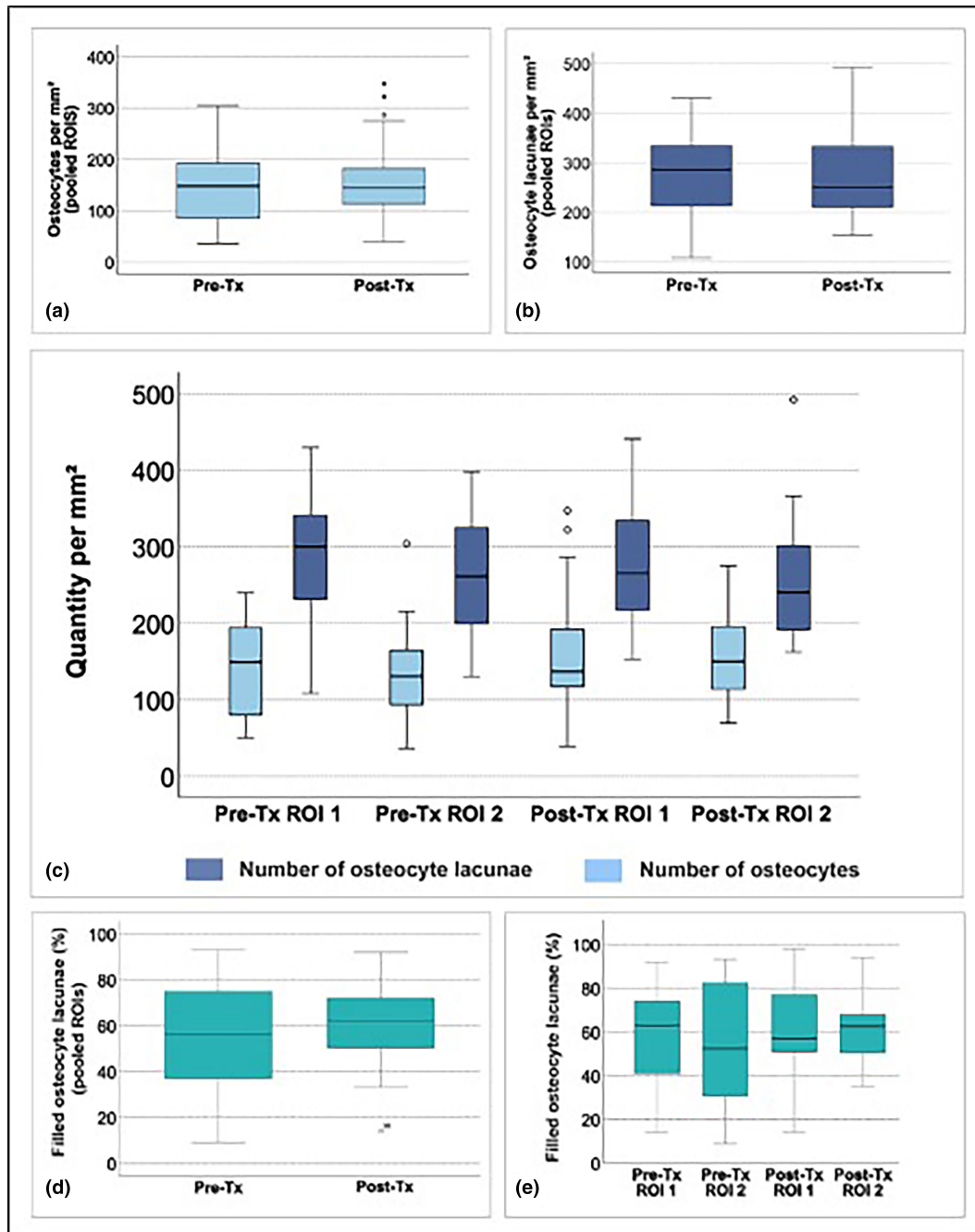


**FIGURE 3** Results for the parameters I. number of osteocytes (light blue), II. number of osteocyte lacunae (dark blue) and III. ratio of filled osteocyte lacunae (green). (a), (b) and (d) show boxplots for the comparison of the Pre-Tx and Post-Tx bone samples (ROIs pooled). (c) and (e) show the boxplots for the comparison of the different ROIs. Post-Tx, post-transplantation/sample after 3 months; Pre-Tx, pre-transplantation/native bone sample; ROI, region of interest.

this timeframe (Fretwurst, Gad, et al., 2015; Fretwurst, Nack, et al., 2015). There is a lack of a two-month and a four-month control group for comparison. However, we included the control group (native bone) at the time of graft harvesting, demonstrating no histological differences. Generally, it is assumed that native/pristine bone is ideal for implant placement.

Grafted cortical bone presents areas of empty osteocyte lacunae, which are considered and quantified as avital/necrotic bone (Acocella et al., 2010; Spin-Neto et al., 2014, 2015). The reduction

of the osteocytes within bone grafts is assumed to be due to a disturbed blood supply after the grafting procedure that causes avascular necrosis with consecutive cell death (Ellegaard et al., 1975; Zerbo et al., 2003). After the blood supply cutoff, ischemia and hypoxia-driven apoptosis of the osteocytes occurs within a few hours, as shown in animal models (Sato et al., 2001; Yuan et al., 2018). Apoptotic osteocytes can induce RANKL-mediated, targeted bone remodeling processes by signaling to adjacent, surviving osteocytes (Kennedy et al., 2014; McCutcheon et al., 2020).

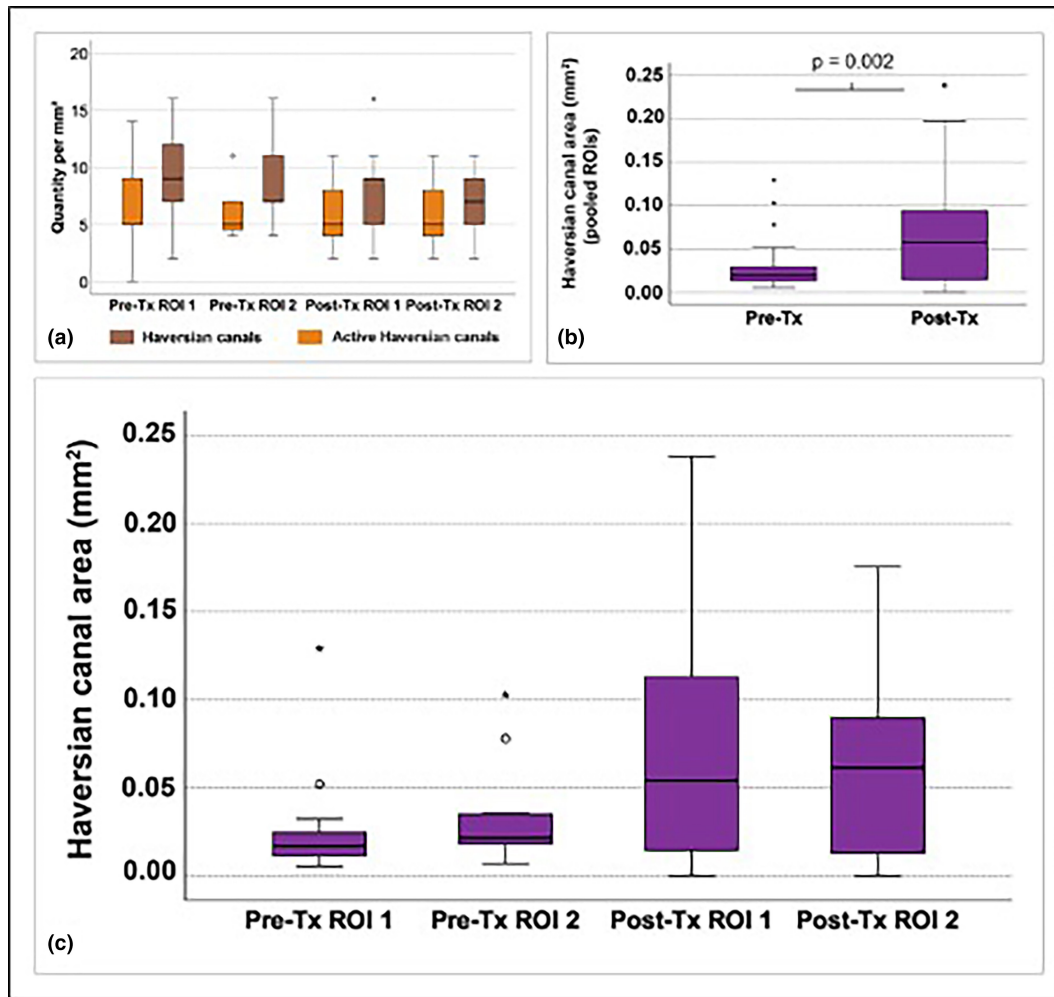


**FIGURE 4** Results for the parameters I. number of Haversian canals (light orange), II. number of active Haversian canals (dark orange) and III. Haversian canal area (purple). (b) shows the boxplots for the comparison of the Pre-Tx and Post-Tx bone samples (ROIs pooled) regarding the Haversian canal area. (a) and (c) show the boxplots for the comparison of the different ROIs. Significant differences ( $p < .05$ ) are indicated by horizontal bars between the boxplots. Post-Tx, post-transplantation/sample after 3 months; Pre-Tx, pre-transplantation/native bone sample; ROI, region of interest.

The osteocyte lacuna exists as long as a viable osteocyte resides within it (Knothe Tate et al., 2004). After osteocyte apoptosis, the lacuna is proposed to be processed (repair/removal) by a basic multicellular unit (BMU) and filled with new bone (Burr, 2014; Hunter & Agnew, 2016).

Animal studies with longitudinal, prospective settings have been conducted but demonstrated heterogeneous results in dependence on the healing period after autologous bone grafting. After a 1-week healing period, Ellegaard et al. demonstrated in a monkey model generalized empty osteocytes lacunae after periodontal autologous bifurcation grafting, while, in contrast, Heslop et al. found in a Wistar rat model a constant number of osteocytes (Ellegaard et al., 1975; Heslop et al., 1960). Autologous bone grafts from the skull showed more than 60% vital bone in a domestic pig model after 2 and 6 months of healing (Moest et al., 2019). After a 6-months healing period, De Santis et al. found histologically no necrotic bone in the incorporated mandibular bone grafts in Labrador dogs (De Santis et al., 2015).

Histological studies in humans demonstrated to exhibit up to 80% of necrotic bone after 3–9 months after autologous bone grafting (Acocella et al., 2010; Spin-Neto et al., 2014) by measuring the surface area within the bone biopsy based on the appearance of the osteocyte lacunae. The data of these studies are not entirely comparable with those of the present study since, in the present work, the bone vitality was assessed based on the number of filled osteocyte lacunae and active Haversian canals and not on the general parameter of the area of the necrotic bone. The present study shows a contradiction to the results or conclusions obtained through earlier studies, as the biopsies retrieved from autologous retromolar bone grafts after incorporation of the graft showed no significant difference regarding the ratio of filled/empty osteocytes lacunae and active/inactive Haversian canals in comparison to the native bone. Notably, on average, more than 50% of osteocyte lacunae appeared filled in all Regions of Interest (ROIs). The grafts appeared to be clinically stable, and vascularized (Acocella et al., 2010; Stricker et al., 2021). This aligns with the observation that the vitality of the

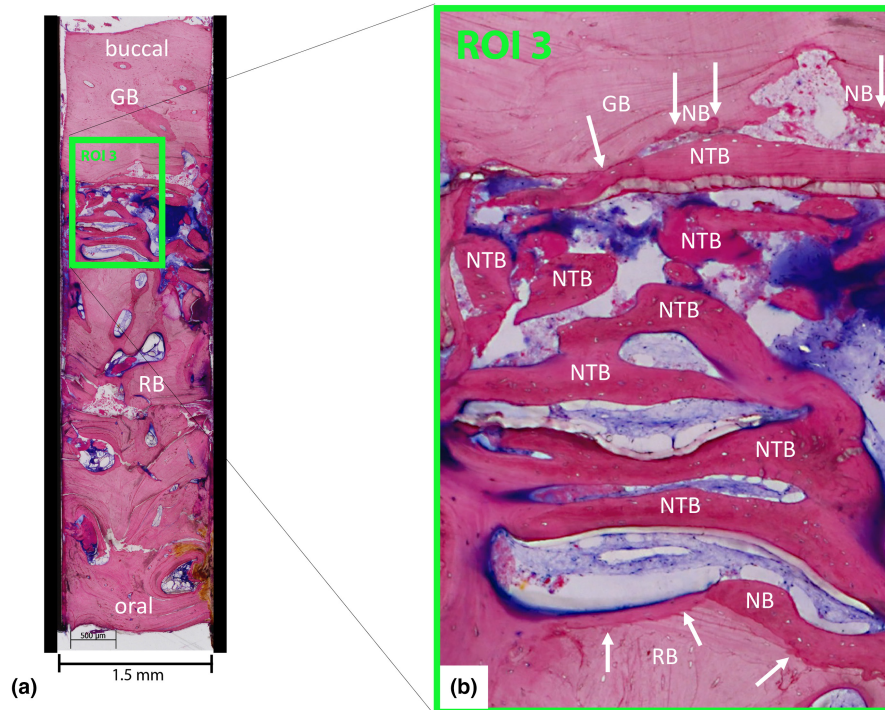


**FIGURE 5** Representative example of one core biopsy illustrating (a) the whole length of the bone biopsy and (b) the border zone between the resident bone (RB) and grafted bone (GB) at higher magnification. Howship's lacunae (arrows) with newly formed bone (NB) on top line the surfaces of resident bone and grafted bone. The border zone in between consists of newly formed trabecular bone (NTB) connecting the two bone parts. Some small fractures and bone fragments (debris) filling part of the bone marrow cavities can be seen. The rectangle in (a) is enlarged in (b).

bone graft, assessed through the parameters measured in this study, demonstrated no significant deviation from its native state at the time of graft removal.

On the other hand the graft stability on the recipient site cannot be measured with histology. The histological appearance of the interfacial zone (ROI 3) demonstrated the continuity of bone tissue in between the donor and recipient site. It should be noted that if bone biopsies taken with the hollow drill are examined histologically, one must expect harvesting artifacts (Cordaro et al., 2008), identify them, and take them into account in the evaluation (Bosshardt, 2014). In the present study, the interface between the local and the grafted bone was particularly affected. During drilling, the cutting edge of the bur produced cracks and fractures in the fragile trabecular network, particularly at the bur–bone interface, and tissue debris particles were pushed from the periphery into the center of the biopsy. Histology clearly shows where the weakest link in the chain is to be found. From a clinical point of view, this finding is important because it indicates that caution is required when preparing the implant bed. It could also indicate that longer healing times are beneficial to give the bone more time to mature.

For the vitality and successful incorporation of a cortical bone graft, in addition to (mechanical) consolidation and substitution by bone from the recipient site, its revascularization is essential (Stevenson et al., 1997). Animal studies demonstrated revascularization of cortical bone grafts after six days (Deleu & Trueta, 1965; Kusiak et al., 1985). The Haversian canal system houses the

vasculature, but within a bone graft, it is also the site of extensive resorptive osteoclastic activity that is organized in “cutting cones” (Agerbaek et al., 1991). It has been proposed that cortical bone grafts are incorporated or revascularized by “creeping substitution”, which describes the gradual resorption of the graft with the simultaneous formation of new bone (Burchardt, 1983; Khan et al., 2005). During this process, a widening of the Haversian canals occurs (Stevenson et al., 1996; Stringa & Mignani, 2014). Although the present study revealed no significant differences between Pre-Tx and Post-Tx bone regarding the quantity of overall Haversian canals and active Haversian canals, it demonstrated that the surface area of the Havers canal within the Post-Tx bone was significantly higher than in the Pre-Tx bone, pointing to the above-mentioned widening of the Haversian canals. Further, the reorganization of bone that occurred after grafting, involving the appearance of cutting cones, which might contribute to the increased surface area of the Haversian canal area.

When using empty or filled osteocyte lacunae as the basis for the measurement of the vitality of the bone, the risk of methodological bias must be acknowledged. The empty/filled osteocyte lacunae ratio can be altered during sample processing by, e.g., fixation, shrinking artifacts, or sectioning (Bauer, 2003). Furthermore, the histological appearance of osteocytes does not confirm the osteocyte activity, the osteogenic potential of the remaining cells or any specific osteocyte network activity. The Haversian canal system represents a three-dimensional construct within the bone, the nature of which cannot be fully visualized in two-dimensional



sections (Bauer, 2003; Taqi et al., 2018). Future research on bone graft incorporation should focus on three-dimensional, minimal to non-destructive methods such as, e.g., Synchrotron micro-CT for the visualization of bone microarchitecture and advanced 3D histological imaging for investigating the function of cells within the bone (Coutu et al., 2017; Rothweiler et al., 2022). It is known that individual factors, such as, e.g., age, gender, in particular sex steroid hormones, can impact bone homeostasis and turnover (Cao et al., 2022; Landwehr et al., 2022; Recker et al., 2018; Shao et al., 2020). Recent proteomics analysis revealed interindividual differences regarding the bone proteome (Fretwurst et al., 2022). Harvesting bone samples from the same patient at different times poses a challenge in planning and clinical implementation. Although the present study succeeded in involving 17 patients, further research on larger and more standardized cohorts must follow to confirm the descriptive results of the present study.

## 5 | CONCLUSION

This study demonstrates, compared to other data, a high rate of vital structures in retromolar bone block grafts after three months of healing, exhibiting the same histological features in comparison to the native alveolar ridge and appearing to be well incorporated into the recipient site. Based on this histomorphometric data, a 3-month healing period seems sufficient for intraoral retromolar bone grafts incorporation prior to dental implant placement. Future studies should explore additional vitality parameters and employ three-dimensional, minimal to nondestructive methods, as the histomorphometry on two-dimensional sections has limitations.

### AUTHOR CONTRIBUTIONS

A.S., K.N., T.F. conceived the ideas. A.S. conducted the surgical procedures and sample acquisition. A.A. performed the histological stainings. A.A., C.G. performed the data extraction. C.G. performed statistics. A.S., K.N., T.F. C.G. interpreted the data. A.S., T.F., and C.G. wrote the manuscript. A.A., F.D., D.B., K.N., D.B., T.A., L.C. contributed to the conception of the work, reviewed, and edited the manuscript, and gave final approval of the version to be published. All authors read and approved the manuscript.

### ACKNOWLEDGMENTS

The authors thank Gerda Siebert and Annette Lindner for supporting histological procedures and data analysis. The authors declare no conflicts of interest with respect to the research, authorship, and publication of this article. The authors do not have any financial interests, either directly or indirectly, related to the products or information discussed in the paper. Open Access funding enabled and organized by Projekt DEAL.

### FUNDING INFORMATION

This study was supported by a grant from Geistlich Biomaterials, Wollhusen/ Switzerland.

### CONFLICT OF INTEREST STATEMENT

The authors declare no conflicts of interest with respect to the research, authorship, and publication of this article. The authors do not have any financial interests, either directly or indirectly, related to the products or information discussed in the paper.

### DATA AVAILABILITY STATEMENT

The data that supports the findings of this study are available in the supplementary material of this article.

### ETHICS STATEMENT

The protocol was approved by the ethics committee of the Albert-Ludwigs-University Freiburg, Germany (Protocol number 138/14). All patients were treated in accordance with the Helsinki Declaration of 1964, as revised in 2013.

### PATIENT CONSENT STATEMENT

All patients were informed about the procedure of the study and have explicitly agreed to participate in the study in written and oral form.

### PERMISSION TO REPRODUCE MATERIAL FROM OTHER SOURCES

No external material reproduced.

### CLINICAL TRIAL REGISTRATION

Commencement date before 31st January 2017.

### ORCID

Andres Stricker  <https://orcid.org/0000-0003-4764-9563>

Tobias Fretwurst  <https://orcid.org/0000-0003-4769-7610>

Tara Aghaloo  <https://orcid.org/0000-0002-2079-5870>

Luca Cordaro  <https://orcid.org/0000-0002-7108-0306>

### REFERENCES

- Acocella, A., Bertolai, R., Colafranceschi, M., & Sacco, R. (2010). Clinical, histological and histomorphometric evaluation of the healing of mandibular ramus bone block grafts for alveolar ridge augmentation before implant placement. *Journal of Cranio-Maxillo-Facial Surgery*, 38, 222–230.
- Agerbaek, M. O., Eriksen, E. F., Kragstrup, J., Mosekilde, L., & Melsen, F. (1991). A reconstruction of the remodelling cycle in normal human cortical iliac bone. *Bone and Mineral*, 12, 101–112.
- Aloy-Prosper, A., Penarrocha-Oltra, D., Penarrocha-Diogo, M., & Penarrocha-Diogo, M. (2015). The outcome of intraoral onlay block bone grafts on alveolar ridge augmentations: A systematic review. *Medicina Oral, Patología Oral y Cirugía Bucal*, 20, e251–e258.
- Ayoubi, M., Tol, A. F., Weinkamer, R., Roschger, P., Brugger, P. C., Berzlanovich, A., Bertinetti, L., Roschger, A., & Fratzl, P. (2021). 3D interrelationship between osteocyte network and forming mineral during human bone remodeling. *Advanced Healthcare Materials*, 10, e2100113.
- Bauer, T. W. (2003). Recognizing and interpreting histology artifacts in hard-tissue research. In Y. H. An & K. L. Martin (Eds.), *Handbook of histology methods for bone and cartilage* (pp. 561–570). Humana Press.

- Bosshardt, D. D. (2014). Histology as a tool to evaluate the outcome of regenerative therapies. In W. V. Giannobile, N. P. Lang, & M. S. Tonetti (Eds.), *Osteology Guidelines for Oral & Maxillofacial Regeneration* (pp. 135–144). Quintessence Publishing.
- Burchardt, H. (1983). The biology of bone graft repair. *Clinical Orthopaedics and Related Research*, (174), 28–42.
- Burger, E. A., Meshkini, H., & Lindeboom, J. A. (2011). One versus two titanium screw fixation of autologous onlay bone grafts in the anterior maxilla: A randomised histological pilot study. *European Journal of Oral Implantology*, 4, 219–225.
- Burr, D. B. (2014). Repair mechanisms for microdamage in bone. *Journal of Bone and Mineral Research*, 29, 2534–2536.
- Buser, D., Dula, K., Hirt, H. P., & Schenk, R. K. (1996). Lateral ridge augmentation using autografts and barrier membranes: A clinical study with 40 partially edentulous patients. *Journal of Oral and Maxillofacial Surgery*, 54, 420–432.
- Cao, B., Liu, M., Luo, Q., Wang, Q., Liu, M., Liang, X., Wu, D., Li, W., Su, C., Chen, J., & Gong, C. (2022). The effect of BMI, age, gender, and pubertal stage on bone turnover markers in Chinese children and adolescents. *Frontiers in Endocrinology*, 13, 1–10.
- Cha, H.-S., Kim, J.-W., Hwang, J.-H., & Ahn, K.-M. (2016). Frequency of bone graft in implant surgery. *Maxillofacial Plastic and Reconstructive Surgery*, 38, 1–4.
- Chen, N. T., Glowacki, J., Bucky, L. P., Hong, H. Z., Kim, W. K., & Yaremchuk, M. J. (1994). The roles of revascularization and resorption on endurance of craniofacial onlay bone grafts in the rabbit. *Plastic and Reconstructive Surgery*, 93, 714–722; discussion 723–4.
- Clementini, M., Morlupi, A., Agrestini, C., & Ottria, L. (2011). Success rate of dental implants inserted in autologous bone graft regenerated areas: A systematic review. *Oral Implantology*, 4, 3–10.
- Cordaro, L., Bosshardt, D. D., Palattella, P., Rao, W., Serino, G., & Chiapasco, M. (2008). Maxillary sinus grafting with bio-Oss or Straumann bone ceramic: Histomorphometric results from a randomized controlled multicenter clinical trial. *Clinical Oral Implants Research*, 19(8), 796–803.
- Cordaro, L., & Terheyden, H. (2014). ITI treatment guide. *Die Quintessenz*, 14–19.
- Coutu, D. L., Kokkaliaris, K. D., Kunz, L., & Schroeder, T. (2017). Three-dimensional map of nonhematopoietic bone and bone-marrow cells and molecules. *Nature Biotechnology*, 35, 1202–1210.
- Cypher, T. J., & Grossman, J. P. (1996). Biological principles of bone graft healing. *The Journal of Foot and Ankle Surgery*, 35, 413–417.
- De Santis, E., Lang, N. P., Favero, G., Beolchini, M., Morelli, F., & Botticelli, D. (2015). Healing at mandibular block-grafted sites. An experimental study in dogs. *Clinical Oral Implants Research*, 26, 516–522.
- Deleu, J., & Trueta, J. (1965). Vascularisation of bone grafts in the anterior chamber of the eye. *Journal of Bone and Joint Surgery. British Volume (London)*, 47, 319–329.
- Ellegaard, B., Karring, T., & Loe, H. (1975). The fate of vital and devitalized bone grafts in the healing of interradicular lesions. *Journal of Periodontal Research*, 10, 88–97.
- Esposito, M., Grusovin, M. G., Felice, P., Karatzopoulos, G., Worthington, H. V., & Coulthard, P. (2009). The efficacy of horizontal and vertical bone augmentation procedures for dental implants – A Cochrane systematic review. *European Journal of Oral Implantology*, 2, 167–184.
- Fretwurst, T., Gad, L. M., Nelson, K., & Schmelzeisen, R. (2015). Dentoalveolar reconstruction: Modern approaches. *Current Opinion in Otolaryngology & Head and Neck Surgery*, 23, 316–322.
- Fretwurst, T., Nack, C., Al-Ghrai, M., Raguse, J., Stricker, A., Schmelzeisen, R., Nelson, K., & Nahles, S. (2015). Long-term retrospective evaluation of the peri-implant bone level in onlay grafted patients with iliac bone from the anterior superior iliac crest. *Journal of Cranio-Maxillo-Facial Surgery*, 43, 956–960.
- Fretwurst, T., Spanou, A., Nelson, K., Wein, M., Steinberg, T., & Stricker, A. (2014). Comparison of four different allogeneic bone grafts for alveolar ridge reconstruction: A preliminary histologic and biochemical analysis. *Oral Surgery, Oral Medicine, Oral Pathology and Oral Radiology*, 118, 424–431.
- Fretwurst, T., Tritschler, I., Rothweiler, R., Nahles, S., Altmann, B., Schilling, O., & Nelson, K. (2022). Proteomic profiling of human bone from different anatomical sites – A pilot study. *Proteomics: Clinical Applications*, 16, e2100049.
- Frost, H. M. (1960). In vivo osteocyte death. *The Journal of Bone and Joint Surgery. American Volume*, 42-A, 138–143.
- Heslop, B. F., Zeiss, I. M., & Nisbet, N. W. (1960). Studies on transference of bone. I. A comparison of autologous and homologous bone implants with reference to osteocyte survival, osteogenesis and host reaction. *British Journal of Experimental Pathology*, 41, 269–287.
- Hunter, R. L., & Agnew, A. M. (2016). Intraskelatal variation in human cortical osteocyte lacunar density: Implications for bone quality assessment. *Bone Reports*, 5, 252–261.
- Kennedy, O. D., Laudier, D. M., Majeska, R. J., Sun, H. B., & Schaffler, M. B. (2014). Osteocyte apoptosis is required for production of osteoclastogenic signals following bone fatigue in vivo. *Bone*, 64, 132–137.
- Khan, S. N., Cammisa, F. P., Jr., Sandhu, H. S., Diwan, A. D., Girardi, F. P., & Lane, J. M. (2005). The biology of bone grafting. *The Journal of the American Academy of Orthopaedic Surgeons*, 13, 77–86.
- Knothe Tate, M. L., Adamson, J. R., Tami, A. E., & Bauer, T. W. (2004). The osteocyte. *The International Journal of Biochemistry & Cell Biology*, 36, 1–8.
- Kusiak, J. F., Zins, J. E., & Whitaker, L. A. (1985). The early revascularization of membranous bone. *Plastic and Reconstructive Surgery*, 76, 510–516.
- Landwehr, V. C., Fretwurst, T., Heinen, J., Vach, K., Nelson, K., Nahles, S., & Iglhaut, G. (2022). Association of sex steroid hormones and new bone formation rate after iliac onlay grafting: A prospective clinical pilot study. *International Journal of Implant Dentistry*, 8, 53.
- Lasckó, J., & Lévai, G. (1975). A simple differential staining method for semi-thin sections of ossifying cartilage and bone tissues embedded in epoxy resin. *Mikroskopie*, 31, 1–4.
- Lassen, N. E., Andersen, T. L., Pløen, G. G., Søre, K., Hauge, E. M., Harving, S., Eschen, G. E. T., & Delaisse, J.-M. (2017). Coupling of bone resorption and formation in real time: New knowledge gained from human haversian Bmus. *Journal of Bone and Mineral Research*, 32, 1395–1405.
- Maggiano, I. S., Maggiano, C. M., Clement, J. G., Thomas, C. D. L., Carter, Y., & Cooper, D. M. L. (2016). Three-dimensional reconstruction of haversian systems in human cortical bone using synchrotron radiation-based micro-CT: Morphology and quantification of branching and transverse connections across age. *Journal of Anatomy*, 228, 719–732.
- Marx, R. E., & Tursun, R. (2012). Suppurative osteomyelitis, bisphosphonate induced osteonecrosis, osteoradionecrosis: A blinded histopathologic comparison and its implications for the mechanism of each disease. *International Journal of Oral and Maxillofacial Surgery*, 41, 283–289.
- McCutcheon, S., Majeska, R. J., Spray, D. C., Schaffler, M. B., & Vazquez, M. (2020). Apoptotic osteocytes induce RANKL production in bystanders via purinergic signaling and activation of pannexin channels. *Journal of Bone and Mineral Research*, 35, 966–977.
- Moest, T., Frabschka, J., Kesting, M. R., Schmitt, C. M., Frohwitter, G., Lutz, R., & Schlegel, K. A. (2019). Osseous ingrowth in allogeneic bone blocks applied for vertical bone augmentation: A preclinical randomised controlled study. *Clinical Oral Investigations*, 24, 2867–2879.
- Nkenke, E., & Neukam, F. W. (2014). Autogenous bone harvesting and grafting in advanced jaw resorption: Morbidity, resorption and

- implant survival. *European Journal of Oral Implantology*, 7(Suppl 2), S203–S217.
- Recker, R. R., Akhter, M. P., Lappe, J. M., & Watson, P. (2018). Bone histomorphometry in transiliac biopsies from 48 normal, healthy men. *Bone*, 111, 109–115.
- Reissmann, D. R., Dietze, B., Vogeler, M., Schmelzeisen, R., & Heydecke, G. (2013). Impact of donor site for bone graft harvesting for dental implants on health-related and oral health-related quality of life. *Clinical Oral Implants Research*, 24, 698–705.
- Rothweiler, R., Gross, C., Bortel, E., Früh, S., Gerber, J., Boller, E., Wüster, J., Stricker, A., Fretwurst, T., Iglhaut, G., Nahles, S., Schmelzeisen, R., Hesse, B., & Nelson, K. (2022). Comparison of the 3D-microstructure between alveolar and iliac bone for enhanced bioinspired bone graft substitutes. *Frontiers in Bioengineering and Biotechnology*, 10, 1–16.
- Sakkas, A., Wilde, F., Heufelder, M., Winter, K., & Schramm, A. (2017). Autogenous bone grafts in oral implantology—is it still a “gold standard”? A consecutive review of 279 patients with 456 clinical procedures. *International Journal of Implant Dentistry*, 3, 23.
- Sanz, M., & Vignoletti, F. (2015). Key aspects on the use of bone substitutes for bone regeneration of edentulous ridges. *Dental Materials*, 31, 640–647.
- Sato, M., Sugano, N., Ohzono, K., Nomura, S., Kitamura, Y., Tsukamoto, Y., & Ogawa, S. (2001). Apoptosis and expression of stress protein (Orp150, Ho1) during development of ischaemic osteonecrosis in the rat. *The Journal of Bone and Joint Surgery*, 83, 751–759.
- Shao, J., Zhou, S.-S., Qu, Y., Liang, B.-B., Yu, Q.-H., & Wu, J. (2020). Correlation between bone turnover and metabolic markers with age and gender: A cross-sectional study of hospital information system data. *BMC Musculoskeletal Disorders*, 21, 603.
- Spin-Neto, R., Stavropoulos, A., Coletti, F. L., Faeda, R. S., Pereira, L. A. V. D., & Marcantonio, E. (2014). Graft incorporation and implant osseointegration following the use of autologous and fresh-frozen allogeneic block bone grafts for lateral ridge augmentation. *Clinical Oral Implants Research*, 25, 226–233.
- Spin-Neto, R., Stavropoulos, A., Coletti, F. L., Pereira, L. A. V. D., Marcantonio, E., & Wenzel, A. (2015). Remodeling of cortical and corticocancellous fresh-frozen allogeneic block bone grafts - a radiographic and histomorphometric comparison to autologous bone grafts. *Clinical Oral Implants Research*, 26, 747–752.
- Starch-Jensen, T., Deluiz, D., Deb, S., Bruun, N. H., & Tinoco, E. M. B. (2020). Harvesting of autogenous bone graft from the ascending mandibular ramus compared with the Chin region: A systematic review and meta-analysis focusing on complications and donor site morbidity. *Journal of Oral and Maxillofacial Research*, 11, e1.
- Stevenson, S., Emery, S. E., & Goldberg, V. M. (1996). Factors affecting bone graft incorporation. *Clinical Orthopaedics and Related Research*, 324, 66–74.
- Stevenson, S., Li, X. Q., Davy, D. T., Klein, L., & Goldberg, V. M. (1997). Critical biological determinants of incorporation of non-vascularized cortical bone grafts. Quantification of a complex process and structure. *The Journal of Bone and Joint Surgery. American Volume*, 79, 1–16.
- Stricker, A., Jacobs, R., Maes, F., Fluegge, T., Vach, K., & Fleiner, J. (2021). Resorption of retromolar bone grafts after alveolar ridge augmentation—Volumetric changes after 12 months assessed by CBCT analysis. *International Journal of Implant Dentistry*, 7, 1–7.
- Stringa, G., & Mignani, G. (2014). Microradiographic investigation of bone grafts in man. *Acta Orthopaedica Scandinavica*, 38, 3–77.
- Taqi, S., Sami, S., Sami, L., & Zaki, S. (2018). A review of artifacts in histopathology. *Journal of Oral and Maxillofacial Pathology*, 22, 1–8.
- Terheyden, H. (2010). Knochenaugmentationen in der Implantologie. *Deutsche Zahnärztliche Zeitung*, 2010(6), 320–330.
- Wang, M., Li, Y., Su, Z., & Mo, A. (2023). Clinical and radiographic outcomes of customized allogeneic bone block versus autogenous bone block for ridge augmentation: 6 month results of a randomized controlled clinical trial. *Journal of Clinical Periodontology*, 50, 22–35.
- Yamada, M., & Egusa, H. (2018). Current bone substitutes for implant dentistry. *Journal of Prosthodontic Research*, 62, 152–161.
- Yuan, H., Jiang, W., Chen, Y., & Kim, B. (2018). Study of osteocyte behavior by high-resolution intravital imaging following photo-induced ischemia. *Molecules*, 23, 1–10.
- Zerbo, I. R., De Lange, G. L., Joldersma, M., Bronckers, A. L., & Burger, E. H. (2003). Fate of monocortical bone blocks grafted in the human maxilla: A histological and histomorphometric study. *Clinical Oral Implants Research*, 14, 759–766.

**How to cite this article:** Stricker, A., Fretwurst, T., Abdullayeva, A., Bosshardt, D., Aghaloo, T., Duttenhöfer, F., Cordaro, L., Nelson, K., & Gross, C. (2024). Vitality of autologous retromolar bone grafts for alveolar ridge augmentation after a 3-months healing period: A prospective histomorphometrical analysis. *Clinical Oral Implants Research*, 00, 1–12. <https://doi.org/10.1111/clr.14306>

## APPENDIX

TABLE A1 *p*-Values and descriptive statistics for differentiated ROIs and pooled ROIs.

	<i>p</i> -Values					
	Nr.OCs	Nr.OCLac	Filled OCLac	Nr.HC	Nr.Active HC	HC Area
Pre-Tx ROI 1						
Pre-Tx ROI 2	1.000	1.000	1.000	1.000	1.000	1.000
Post-Tx ROI 1	1.000	1.000	1.000	1.000	1.000	.059
Post-Tx ROI 2	1.000	1.000	1.000	.752	1.000	.244
Pre-Tx ROI 2						
Pre-Tx ROI 1	1.000	1.000	1.000	1.000	1.000	1.000
Post-Tx ROI 1	1.000	1.000	1.000	1.000	1.000	.391
Post-Tx ROI 2	1.000	1.000	1.000	1.000	1.000	1.000
Post-Tx ROI 1						
Pre-Tx ROI 1	1.000	1.000	1.000	1.000	1.000	.059
Pre-Tx ROI 2	1.000	1.000	1.000	1.000	1.000	.391
Post-Tx ROI 2	1.000	1.000	1.000	1.000	1.000	1.000
Post-Tx ROI 2						
Pre-Tx ROI 1	1.000	1.000	1.000	0.752	1.000	.244
Pre-Tx ROI 2	1.000	1.000	1.000	1.000	1.000	1.000
Post-Tx ROI 1	1.000	1.000	1.000	1.000	1.000	1.000
Pre- vs. Post-Tx (ROIs pooled)	.413	.611	.467	.074	.495	<b>.002</b>
	Descriptives					
	Mean	Median	Interquartile Range	Std. Deviation	Minimum	Maximum
Nr.OCs (per mm <sup>2</sup> )						
Pre-Tx	143.36	148.00	110.00	65.37	36	304
Post-Tx	161.19	144.00	82.00	73.74	39	347
Nr.OCLac (per mm <sup>2</sup> )						
Pre-Tx	276.46	286.00	130.00	80.63	108	430
Post-Tx	271.97	251.00	130.00	87.82	153	492
Filled OCLac (%)						
Pre-Tx	55.20	56.35	39.23	24.46	8.9	92.9
Post-Tx	59.70	61.70	23.40	18.10	13.80	91.50
Nr.HC (per mm <sup>2</sup> )						
Pre-Tx	8.96	8.96	5.00	3.47	2	16
Post-Tx	7.48	7.48	4.00	3.10	2	16
Nr.Active HC (per mm <sup>2</sup> )						
Pre-Tx	6.18	6.18	4.00	3.14	0	14
Post-Tx	5.84	5.84	5.00	2.75	2	11
HC Area (mm <sup>2</sup> )						
Pre-Tx	0.029	0.020	0.018	0.029	0.005	0.129
Post-Tx	0.069	0.058	0.089	0.060	0.000	0.238

Note: *p*-Values as resulted from ANOVA and Bonferroni post-hoc testing (differentiated ROIs) and Mann-Whitney *U* (two-tailed *p*-values, pooled ROIs). *p*-Values <.005 are marked in bold.

Abbreviations: HC, Haversian canals; OC, number of osteocytes; OCLac, osteocyte lacunae; ROI, region of interest; Tx, transplantation.